Tin-containing silicates

structure–activity relations

Osmundsen, Christian M.; Holm, Martin Spangsberg; Dahl, Søren; Taarning, Esben

Published in:
Proceedings of the Royal Society A: Mathematical, Physical and Engineering Sciences

Link to article, DOI:
10.1098/rspa.2012.0047

Publication date:
2012

Document Version
Publisher's PDF, also known as Version of record

PROCEEDINGS OF THE ROYAL SOCIETY A MATHEMATICAL, PHYSICAL & ENGINEERING SCIENCES

Tin-containing silicates: structure–activity relations

Christian M. Osmundsen, Martin Spangsberg Holm, Søren Dahl and Esben Taarning

Proc. R. Soc. A 2012 **468**, 2000-2016 first published online 29 February 2012
doi: 10.1098/rspa.2012.0047

PROCEEDINGS OF THE ROYAL SOCIETY A

Proc. R. Soc. A (2012) **468**, 2000–2016
doi:10.1098/rspa.2012.0047
Published online 29 February 2012

Tin-containing silicates: structure–activity relations

By Christian M. Osmundsen[1,2], Martin Spangsberg Holm[1], Søren Dahl[2] and Esben Taarning[1,*]

[1]*Research and Development Division, Haldor Topsøe A/S, Nymøllevej 55, 2800 Kgs., Lyngby, Denmark*
[2]*Department of Physics, Technical University of Denmark, Lyngby, Denmark*

The selective conversion of biomass-derived substrates is one of the major challenges facing the chemical industry. Recently, stannosilicates have been employed as highly active and selective Lewis acid catalysts for a number of industrially relevant reactions. In the present work, four different stannosilicates have been investigated: Sn-BEA, Sn-MFI, Sn-MCM-41 and Sn-SBA-15. When comparing the properties of tin sites in the structures, substantial differences are observed. Sn-beta displays the highest Lewis acid strength, as measured by probe molecule studies using infrared spectroscopy, which gives it a significantly higher activity at low temperatures than the other structures investigated. Furthermore, the increased acid strength translates into large differences in selectivity between the catalysts, thus demonstrating the influence of the structure on the active site, and pointing the way forward for tailoring the active site to the desired reaction.

Keywords: stannosilicate; biomass; catalysis; zeolite; infrared

1. Introduction

The selective conversion of biomass to fuels and chemicals is one of the major challenges facing the chemical industry in the twenty-first century (Ragauskas *et al.* 2006). Owing to the significantly different nature of biomass compared with fossil resources, current conversion technologies cannot be directly applied and new catalytic systems and catalysts need to be developed (Christensen *et al.* 2008; Vennestrøm *et al.* 2011). In this regard, stannosilicates have recently attracted significant attention as highly active and selective Lewis acid catalysts in a number of reactions involving biomass-derived substrates, such as monosaccharide isomerization (Moliner *et al.* 2010; Román-Leshkov *et al.* 2010; Nikolla *et al.* 2011), retro aldol condensations (Holm *et al.* 2010), hydride shifts (Taarning *et al.* 2009; Holm *et al.* 2010; Li, L. *et al.* 2011), as well as a number of other reactions including Meerwein–Ponndorf–Verley–Oppenauer (MPVO) redox reactions (Corma *et al.* 2002, 2003; Boronat *et al.* 2006*a*,*b*; Sasidharan *et al.* 2009) and Baeyer–Villiger oxidations (Boronat *et al.* 2005, 2006*b*, 2009; Sasidharan *et al.* 2009; Li, P. *et al.* 2011). In particular, tin atoms incorporated in zeolite beta have

*Author for correspondence (esta@topsoe.dk).

One contribution of 14 to a Special feature ‘Recent advances in single-site heterogeneous catalysis’.

Received 1 December 2011
Accepted 1 February 2012

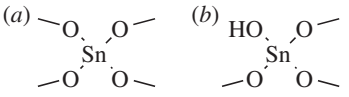

Figure 1. Tin sites in zeolite Sn-beta: (*a*) isomorphously substituted and (*b*) partially hydrolysed.

been shown to be highly active sites for these reactions; however, owing to the difficulty in preparing Sn-beta, other materials have been investigated, such as the mesoporous stannosilicate Sn-MCM-41 (Li, L. *et al.* 2011).

The incorporation of acid functionality in silicates is most well known with the incorporation of aluminium in zeolites to impart Brønsted acidity. Several other heteroelements, such as Ti, Zr, Sn, Nb, Ta and V (Taramasso *et al.* 1983; Valencia & Corma 2001; Corma *et al.* 2003, 2009; Zhu *et al.* 2004; de la Torre *et al.* 2010), have been incorporated in zeolite structures, but these elements do not introduce a charge imbalance like that responsible for the Brønsted acidic behaviour of aluminium-containing zeolites. In some cases, other functionalities can arise, such as the ability of titanium silicalite-1 (TS-1) to catalyse epoxidations (Thomas *et al.* 2005; Fan *et al.* 2009). The incorporation of isolated tin atoms has been shown to impart a strong Lewis acid functionality to silicates (Corma *et al.* 2003). The tin atoms, substitute individual silicon atoms, giving rise to electron-deficient active sites, which are able to coordinate to an electron donor, e.g. the carbonyl oxygen of carbohydrates. Although direct isomorphous substitution of silicon with tin is possible, several studies (Boronat *et al.* 2005, 2006*a*, 2007, 2009) have shown that the active site in Sn-beta is partially hydrolysed, as shown in figure 1. It has further been claimed that the hydroxyl group acts as a base, thereby creating a bifunctional active site, critical for the activity of the catalyst (Boronat *et al.* 2007).

Furthermore, the partial hydrolysis of the tin site increases the Lewis acidity of the tin site; a thesis that has been corroborated by both theoretical calculations and experimental observations (Boronat *et al.* 2005). Whether other stannosilicates possess several distinct tin sites in a similar fashion is less clear. Studies of probe molecules dosed onto Sn-MCM-41 have indicated that, in addition to the sites present in Sn-beta, doubly hydrolysed tin sites are also present (Boronat *et al.* 2009). Conversely, in Sn-MFI, only fully incorporated tin atoms were observed (Boronat *et al.* 2009). Although the catalytic properties of stannosilicates differ significantly between structures, no thorough understanding of the nature or causes of these differences has been developed—an understanding that is necessary for the design of improved catalysts (Thomas *et al.* 2005, 2009). Thus, the present work focuses on the comparison of different stannosilicates in a range of carbohydrate conversion reactions, and on relating these results to the Lewis acidity of the active sites as measured by infrared (IR) spectroscopy to elucidate the effect of the structure on the catalytic properties of the materials.

2. Experimental

Tin atoms were incorporated into the framework of zeolites silicalite-1 (MFI) and beta (BEA), with a Si/Sn ratio of 200. Furthermore, two mesoporous stannosilicates, MCM-41 and SBA-15, were prepared with tin atoms incorporated in the structure with Si/Sn ratios of 50 and 200, respectively.

Sn-BEA (Holm *et al.* 2010) was prepared by mixing 29.0 g of tetraethylammonium hydroxide (TEAOH; 40 wt.%) with 4.0 g of water. To this mixture, 30.6 g of tetraethyl orthosilicate (TEOS), was added and the mixture was stirred for 90 min. A solution of 0.26 g of $SnCl_4 \cdot 5H_2O$ in 4.0 g of water was added slowly. The mixture was stirred to allow the TEOS to hydrolyse and the formed ethanol to evaporate. A mixture of 3.1 g of HF (47–51 wt.%) and 3.0 g of water was added slowly, forming a white rigid gel. A suspension of 0.36 g of dealuminated zeolite beta seeds, prepared according to the procedure described in the patent of Valencia & Corma (2001), in 3.0 g of water was mixed with the synthesis gel. The final gel had an approximate composition of 1 Si : 0.005 Sn : 0.5 TEA^+ : 0.5 F^- : 8 H_2O. The gel was transferred to a Teflon-lined autoclave and crystallized at 140°C for 12 days.

Sn-MFI (Mal *et al.* 1997) was prepared by dissolving 5.35 g of NH_4F in 25.0 g of water. A solution of 0.25 g of $SnCl_4 \cdot 5H_2O$ in 10.0 g of water was added slowly with rapid stirring, followed by a solution of 9.8 g of tetrapropylammonium bromide (TPABr) in 56.0 g of water. In this mixture, 8.6 g of fumed silica was dissolved. The mixture was stirred for 3 h to yield a gel with the approximate composition of 1 Si : 0.005 Sn : 0.26 TPA^+ : 1 F^- : 35 H_2O. The gel was transferred to a Teflon-lined autoclave and crystallized at 200°C for 6 days.

Sn-MCM-41 (Li, L. *et al.* 2011) was prepared by dissolving 13.0 g of hexadecyltrimethylammonium bromide (CTAB) in 38.0 g of water. To this solution of 26.4 g of tetramethylammonium silicate (TMAS; 15–20 wt.%) was added slowly, and the mixture was stirred for 50 min. The desired amount of $SnCl_4 \cdot 5H_2O$ and HCl (37 wt.%) was dissolved in 2.1 g of water and the solution added slowly. The mixture was stirred for a further 1.5 h, at which point 12.2 g of TEOS was added. The mixture was stirred for 3 h to give a gel with an approximate composition of 1 Si : X Sn : 0.44 CTAB : 0.27 TMA : 0.08 Cl^- : 46 H_2O, with X being either 0.02 or 0.005. The gel was transferred to a Teflon-lined autoclave and heated to 140°C for 15 h.

SBA-15 (Ramaswamy *et al.* 2008) was prepared by dissolving 8.0 g of Pluronic P-123 (PEG-PPG-PEG polymer, $Mw = 5800\,g\,mol^{-1}$) in 60.0 g of water. A solution of 1.0 g of HCl (37 wt.%) in 140 g of water was added, and the mixture stirred for 2 h. Then, 18.0 g of TEOS and the desired amount of $SnCl_4 \cdot 5H_2O$ dissolved in 2.0 g of water was added slowly. The mixture was stirred for 24 h at 40°C to give a gel with an approximate composition of 1 Si : X Sn : 0.016 P123 : (0.12 + X) Cl^- : 134 H_2O, with X being either 0.005 or 0.02. The gel was transferred to a Teflon-lined autoclave and heated to 100°C for 24 h.

All of the catalysts were isolated by suction filtration and washed with ample water. The catalysts were dried overnight at 80°C and calcined in static air at 550°C for 10 h (heating rate: 2°C min^{-1}).

The diffraction pattern of the samples was measured by powder X-ray diffraction on a Phillips X'Pert diffractometer using Cu-Kα radiation. The elemental composition of the solid materials was determined by atomic emission spectroscopy (ICP-OES) measured on a Perkin Elmer model Optima 3000, Varian Vista. Elemental analysis of reaction liquids was performed on an Agilent 7500ce ICP-MS. Pore volume and surface area measurements were performed by multipoint N_2 adsorption/desorption on a Quantachrome Autosorb automatic surface area and pore size analyser. The surface area and micropore volume were calculated using the BET and *t*-plot methods, respectively. The computer

program AUTOSORB 3 was used for the data treatment. SEM pictures were taken with a Quanta scanning electron microscope. The samples were made conductive by depositing a silver layer. Measurements of the IR spectra of the samples were performed on a BioRad FTS 80 spectrometer equipped with an MCT detector operated in transmission mode. The samples were pressed into self-supporting wafers and mounted in a Pyrex measurement cell with NaCl windows that was connected to a vacuum line. Samples were dehydrated before analysis at 375°C for at least 2 h. Probe molecule studies were performed by subjecting the sample to small aliquots of deuterated acetonitrile. The probe molecule was then slowly desorbed by subjecting the sample to reduced pressure for short periods of time, and the spectrum recorded between each desorption.

The conversion of triose sugars to methyl lactate was performed by dissolving 110 mg of the triose dimer, either 1,3-dihydroxyacetone (DHA) or glyceraldehyde (GLA), in 4.0 g of methanol. A total of 80 mg of catalyst was added and the mixture sealed in a glass vial and heated to the desired reaction temperature. The reaction was allowed to proceed for 24 h with stirring. A blank experiment was performed with purely siliceous zeolite beta.

To test the conversion of sucrose to methyl lactate, 450 mg of sucrose was dissolved in 15.0 g of methanol and 150 mg of catalyst was added. The mixture was sealed in a stirred autoclave and heated to 160°C for 16 h. A blank experiment was performed with purely siliceous zeolite beta. The spent catalyst was regenerated by calcination at 550°C for 10 h.

The isomerization of glucose to fructose was performed by adding 50 mg of catalyst to 5.0 g of a glucose solution (2 wt.% in water or 1 wt.% in methanol). The mixture was sealed in a glass vial and heated to the desired reaction temperature with stirring. Individual experiments were performed for different sampling times.

After reaction, the catalyst was removed using a syringe filter, and the reaction mixtures were analysed by gas chromatography (GC) and high-performance liquid chromatography (HPLC). Methyl lactate was quantified by GC analysis on an Agilent 7890A gas chromatograph equipped with an HP-Innowax column and a flame ionization detector. All other compounds were separated by HPLC on an Agilent 1200 series liquid chromatograph equipped with an Aminex HPX-87H column operating at 65°C. The eluent was 0.004 M H_2SO_4 with a flow rate of 0.6 ml min^{-1}. The analytes were quantified with an refractive index detector. The column did not produce adequate separation of fructose and mannose; however, as the response factors of the two compounds are nearly identical, they were treated as a single compound, and quantified with the response factor of fructose. Owing to the acidic eluent, all acetals present in the reaction liquids were hydrolysed and thus quantified as such.

3. Results and discussion

The diffraction patterns of the zeolites, shown in figure 2, confirm that zeolites MFI and BEA have been formed with a high degree of crystallinity. No unassigned diffraction lines corresponding to tin oxide were observed. The diffraction patterns of the mesoporous stannosilicates (not shown) clearly demonstrate the amorphous nature of the samples as no diffraction lines were observed at angles higher than 5°. At lower angles, shown in figure 3, diffraction lines corresponding to

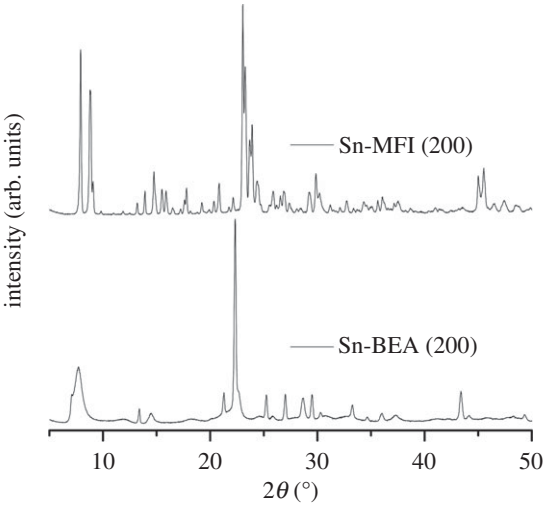

Figure 2. Diffraction pattern of the zeolites.

the (100), (110) and (200) reflections were observed, arising from the order of the mesopores. The measured angles correspond to a d_{100} spacing of roughly 106 Å for the SBA-15 structures and 41 Å for the MCM-41 structures. A slight increase in the *d*-spacing is observed with increasing tin content for both structures. These results are in good agreement with previously reported values (Selvaraj & Choe 2010; Li, L. *et al.* 2011). Measurements of the surface area and pore volume of the materials further confirmed that highly porous structures had been formed, in agreement with the expected structures. Elemental analysis shows a high degree of incorporation of tin in the zeolite structures; however, in the case of the mesoporous stannosilicates, the incorporation varied significantly (table 1).

SEM pictures of the materials (figure 4) show distinctly different morphologies. The Sn-BEA crystals are very small (less than 1 µm) spherical particles, while Sn-MFI has large coffin-shaped crystals with a length in excess of 20 µm. The large particle size in combination with the narrow pore system of the MFI structure means that severe diffusion limitations must be expected for this catalyst. The appearance of the mesoporous stannosilicates also differs significantly; Sn-MCM-41 does not appear to have a distinct particle shape, which is not surprising owing to the amorphous nature of the sample. Sn-SBA-15, on the other hand, presents as hexagonal discs. This particle shape seems to fit well with the two-dimensional hexagonal ordering of the pore system in SBA-15.

The IR spectra taken of the zeolites (not shown) do not display any significant band around 3700 cm^{-1}, which is assigned to framework defects, indicating a very low defect concentration, as expected for zeolites prepared by the fluoride route. The IR spectra of deuterated acetonitrile dosed onto the materials are shown in figure 5. All of the spectra display a prominent band at approximately 2275 cm^{-1}, arising from acetonitrile interacting with the silanol groups of the material, and a second band at 2266 cm^{-1}, which is caused by physisorbed acetonitrile (Boronat *et al.* 2005). For the mesoporous stannosilicates, the second band was only observed at very high loadings of acetonitrile (not shown). The bands caused

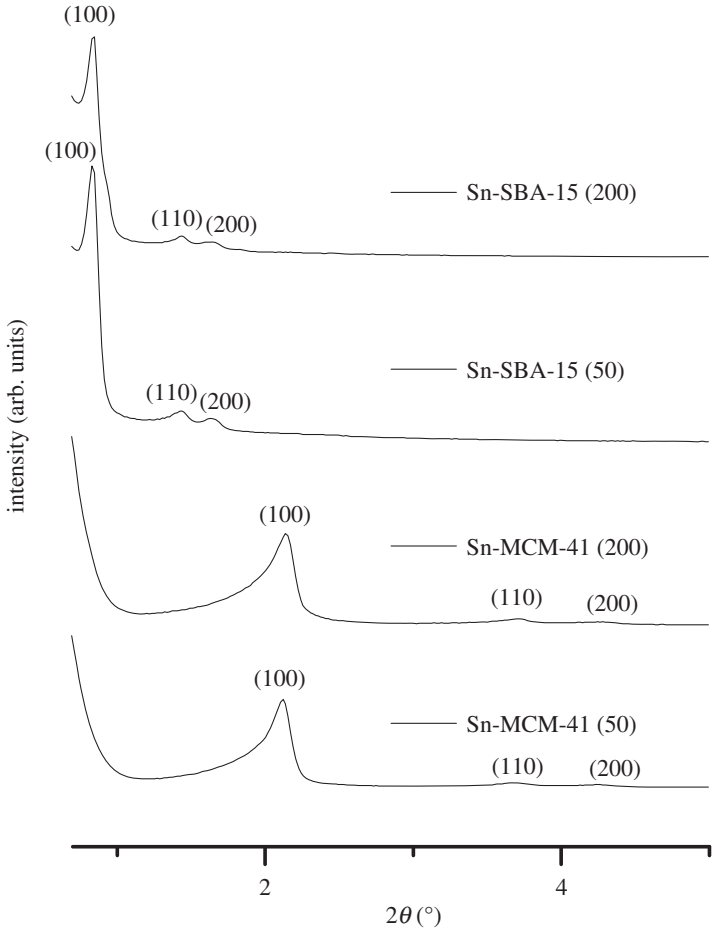

Figure 3. Diffraction pattern of the mesoporous stannosilicates.

Table 1. Characterization of the prepared materials.

	chemical analysis		surface area ($m^2\,g^{-1}$)		pore volume ($ml\,g^{-1}$)	
sample	Sn (wt.%)	DOI[a] (%)	BET	micro-pore[b]	total	micro-pore[b]
Sn-BEA (200)	0.86	87	480	390	0.29	0.20
Sn-MFI (200)	0.82	82	365	190	0.20	0.10
Sn-MCM-41 (50)	2.70	68	1245	0	1.29	0
Sn-MCM-41 (200)	0.49	49	1114	0	1.26	0
Sn-SBA-15 (50)	0.99	25	1229	24	1.67	0.01
Sn-SBA-15 (200)	0.61	61	1354	52	1.80	0.03

[a]Degree of insertion; the ratio of Sn atoms detected by chemical analysis to the amount in the synthesis mixture.
[b]Determined using the *t*-plot method.

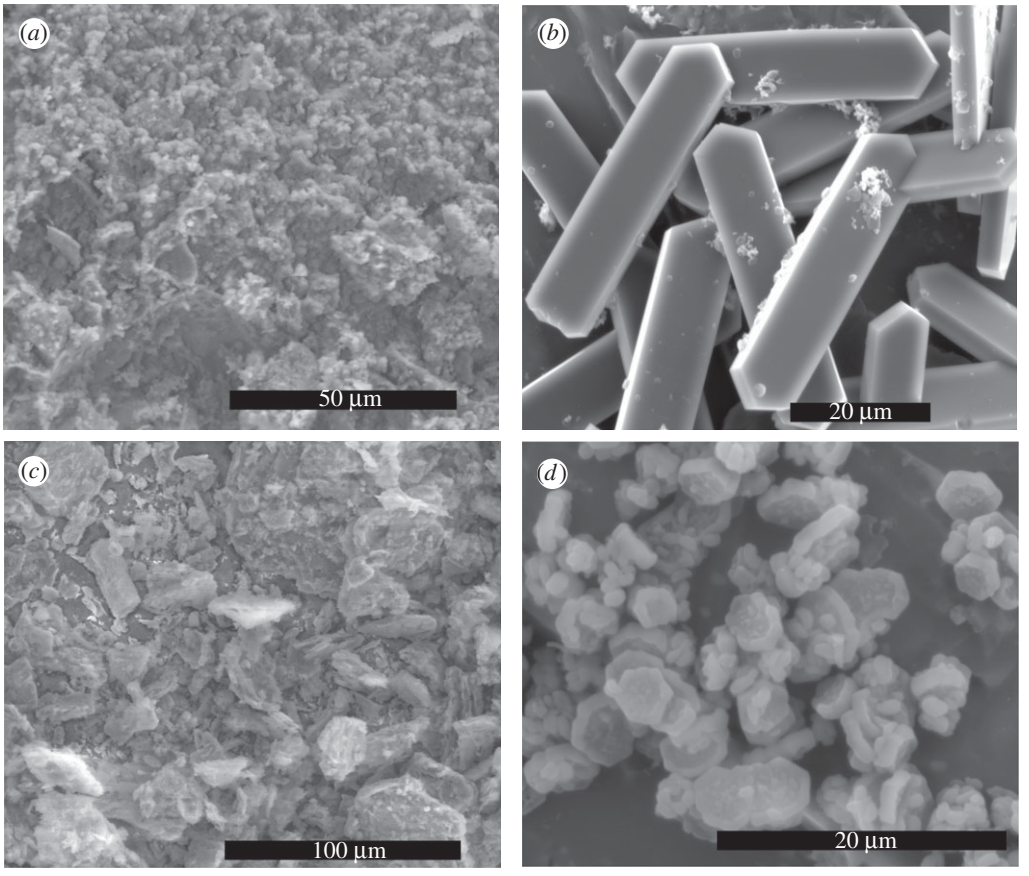

Figure 4. Representative SEM pictures of the catalyst samples. (*a*) Sn-BEA (200), (*b*) Sn-MFI (200), (*c*) Sn-MCM-41 (50) and (*d*) Sn-SBA-15 (50).

by the tin sites were in the region 2305–2320 cm^{-1}. For Sn-BEA, two distinct bands were observed at 2308 and 2317 cm^{-1}, corresponding to the isomorphously substituted and hydrolysed tin sites, respectively (Boronat *et al.* 2005). The difference in adsorption strength between the sites is clearly seen in the difference in desorption rate; the intensity of the band arising from the isomorphously substituted site is rapidly reduced upon exposure to reduced pressure, while the other band remains virtually unchanged. A similar appearance is not observed for the other catalysts.

For Sn-MFI, a single band at 2310 cm^{-1} was observed and a small band at 2290 cm^{-1}. The band at 2310 cm^{-1} probably arises from isomorphously substituted tin, as is observed in Sn-BEA, but the lack of a band at higher wavenumbers indicates that the hydrolysed tin site is not present to any significant degree, demonstrating a significant difference between the BEA and MFI frameworks. The band at 2290 cm^{-1} is unassigned, and it is thus not known whether this arises from a tin site or defects in the structure. The spectra of the two mesoporous stannosilicates look very similar, which is not surprising as the main difference between the structures is the size of the pores. They both

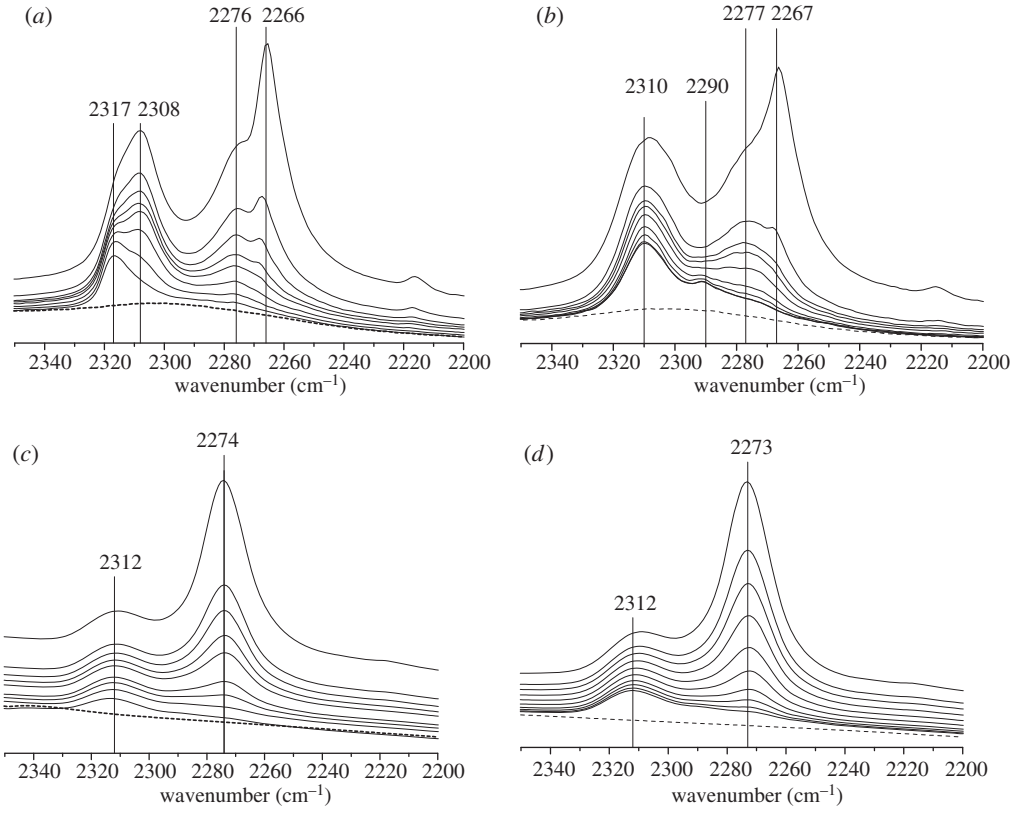

Figure 5. IR spectra of acetonitrile dosed onto the catalyst samples and then successively desorbed. (*a*) Sn-BEA (200), (*b*) Sn-MFI (200), (*c*) Sn-MCM-41 (50) and (*d*) Sn-SBA-15 (50). The intensities have not been normalized and should therefore only be interpreted qualitatively. The dashed line is the zeolite before adsorption of the probe molecule.

display a broad band centred at 2312 cm^{-1}. Since the tin atoms are inserted in an amorphous structure, one would expect a broad range of possible local bonding arrangements, leading to a large variation in Lewis acid strength for the tin sites in the mesoporous stannosilicates, in agreement with the observed spectra. In this case, one would, however, also expect that the maximum of the band would gradually shift to higher wavenumbers as the probe molecules are desorbed (as is observed clearly for Sn-BEA) as the rate of desorption would be higher from the weaker sites. This does not appear to be the case, however—judging the adsorption strength simply from the observed shift may be an oversimplification.

Lactic acid is an important commodity chemical currently produced from carbohydrates by fermentation. The number of potential uses of lactic acid is vast (Gandini 2008; Serrano-Ruiz & Dumesic 2009; Pereira *et al.* 2011); however, the current relatively high price precludes many of these applications, thus improved processes for the production of lactic acid would be of great interest. An alternative catalytic process has been demonstrated, where lactic acid derivatives are prepared by the combined isomerization/esterification of triose sugars with a Lewis acid catalyst (Hayashi & Sasaki 2005; Janssen *et al.* 2007; Taarning *et al.*

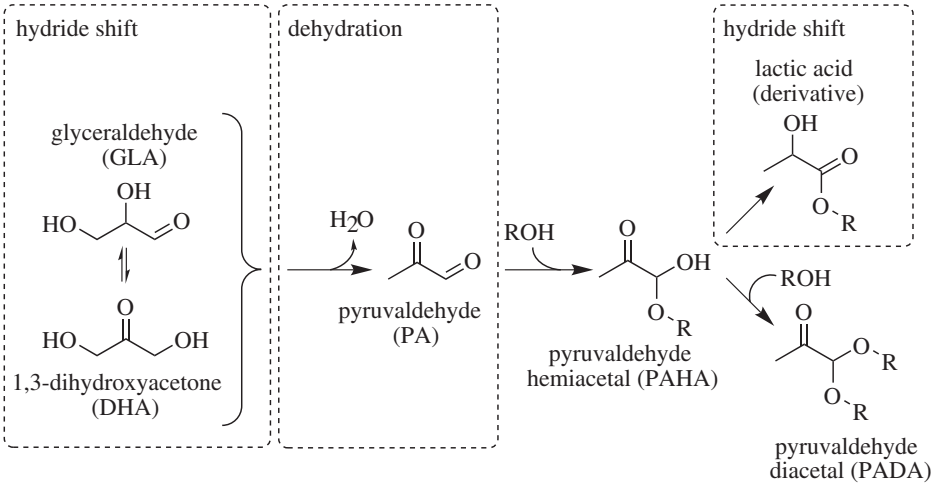

Figure 6. Tentative reaction scheme for the conversion of triose sugars to lactic acid (derivatives).

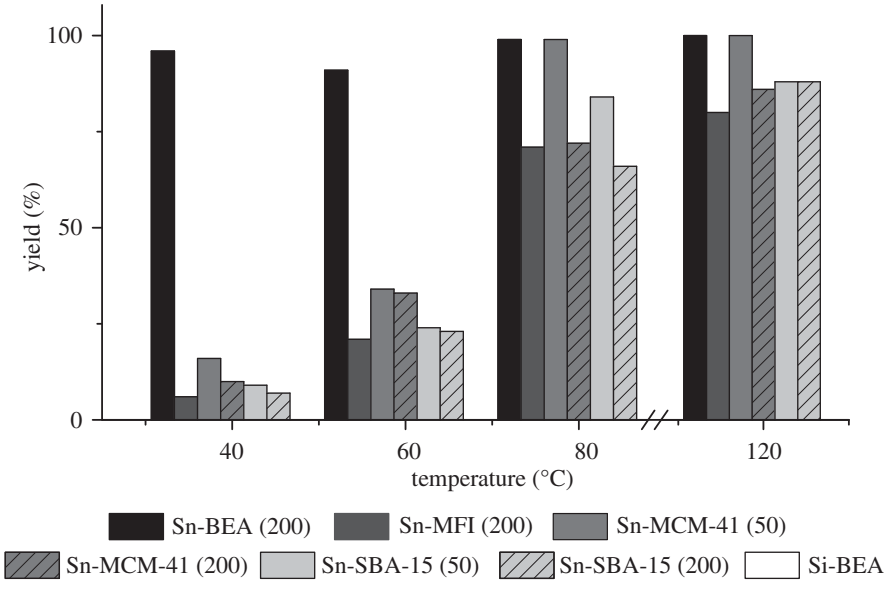

Figure 7. Yield of methyl lactate from the isomerization/esterification of DHA in methanol. Si-BEA did not produce methyl lactate at any temperature.

2009; West *et al.* 2010; Li, L. *et al.* 2011; Zehui & Zongbao 2011). The reaction scheme is given in figure 6. The conversion was investigated over a wide range of temperatures with the prepared stannosilicate catalysts; the obtained yields are given in figure 7. As can be seen, at 120°C, all catalysts give high yields of methyl lactate (greater than 80%). The major compounds in the reaction mixture besides the product are the intermediate pyruvaldehyde (PA), present as the hemiacetal (PAHA), and the trioses. One of the major by-products typically produced is the diacetal PADA, formed by the Brønsted acid-catalysed second

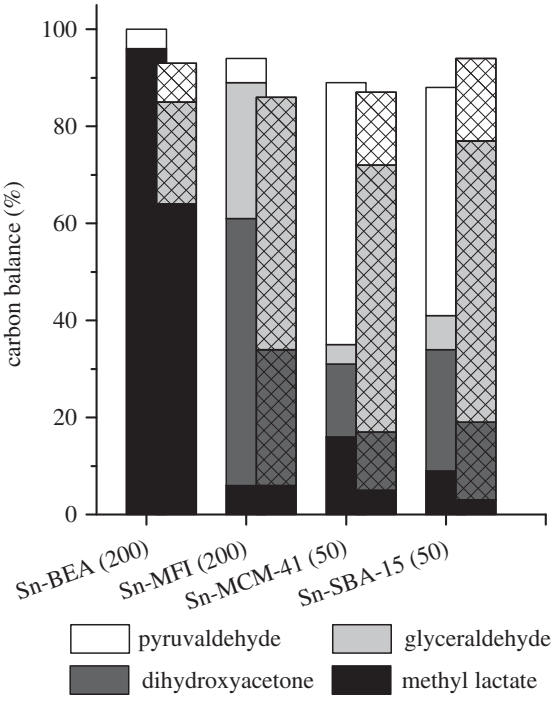

Figure 8. Product mixture from the isomerization/esterification of DHA (no cross-hatching) or GLA (cross-hatching) at 40°C.

pathway shown in figure 6; however, this was not present in significant quantities. At a reaction temperature of 40°C, near quantitative yields are obtained with Sn-BEA, which is significantly better than all other tested catalysts, which gave less than 20 per cent. It is unlikely that this difference can be explained simply in terms of a higher number of active sites in the catalyst, but rather indicates that the active sites in Sn-BEA are capable of activating the substrate to a much greater extent. Even at 80°C, only Sn-MCM-41 (50) is able to give quantitative yields; however, this requires a tin content in the structure three times higher than in Sn-BEA. Using the bulk tin content of the samples as a measure of the number of active sites should however be done with great care, as the distribution between different types of sites is not necessarily identical between the structures, and furthermore, especially in the case of the mesoporous stannosilicates, not all tin atoms are necessarily accessible from the pore system. Finally, the effect of diffusion limitations should not be overlooked, although this will probably have a limited effect for this reaction owing to the small size of the substrate.

In figure 8, the composition of the product mixture obtained from the conversion of trioses at 40°C is given. It is very surprising to note the difference in distribution between the intermediates: for the Sn-SBA-15 and Sn-MCM-41 catalysts (and for Sn-BEA, although the high yield makes it difficult to conclude) the main intermediate is PA; however, for Sn-MFI, only relatively low amounts of this intermediate are present. Instead, a significantly larger fraction is present as the corresponding triose isomer of the substrate. The first step in the conversion of trioses to methyl lactate is the dehydration of the triose to PA, which appears to

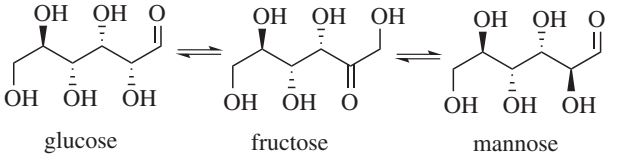

Figure 9. Reaction scheme for the isomerization of glucose.

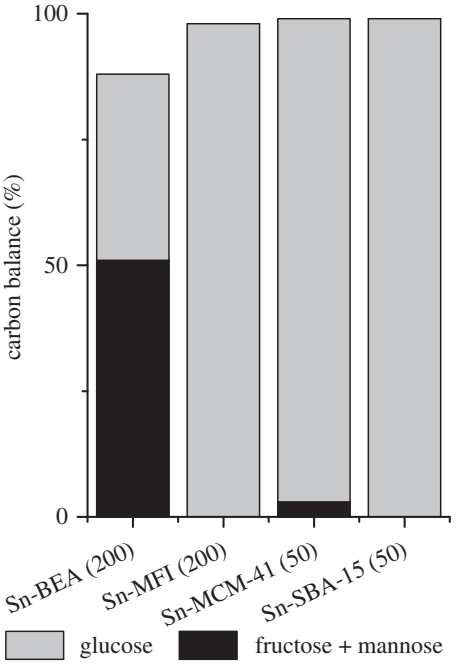

Figure 10. Distribution between hexoses after 48 h of reaction at 80°C in water.

proceed rapidly for the SBA-15 and MCM-41 catalysts, followed by the formation of the PAHA. The significant amount of PAHA present indicates that the rate-limiting step is the hydride shift to yield methyl lactate. Conversely, for Sn-MFI, the large amount of the corresponding triose, and low amount of PAHA, indicates that the hydride shift to yield methyl lactate from PAHA and to interconvert the trioses is relatively fast and the rate-limiting step is instead the dehydration of the triose sugars. This difference in selectivity displayed by tin sites in different structures shows that the activity of the active sites cannot simply be judged from the strength of the Lewis acid sites, and may in fact indicate that different active sites are responsible for the dehydration and hydride shift reactions.

Sn-BEA is an effective catalyst for the isomerization of glucose to fructose and mannose in water (reaction scheme shown in figure 9; Moliner *et al.* (2010)). The isomerization was performed with a reaction time of 48 h and a reaction temperature of 80°C. The results are given figure 10. As can be seen, only Sn-BEA is capable of effectively catalysing the conversion; while Sn-BEA reached the equilibrium distribution within 8 h, none of the other catalysts was able to obtain conversions higher than 5 per cent in 48 h. The low conversion obtained by

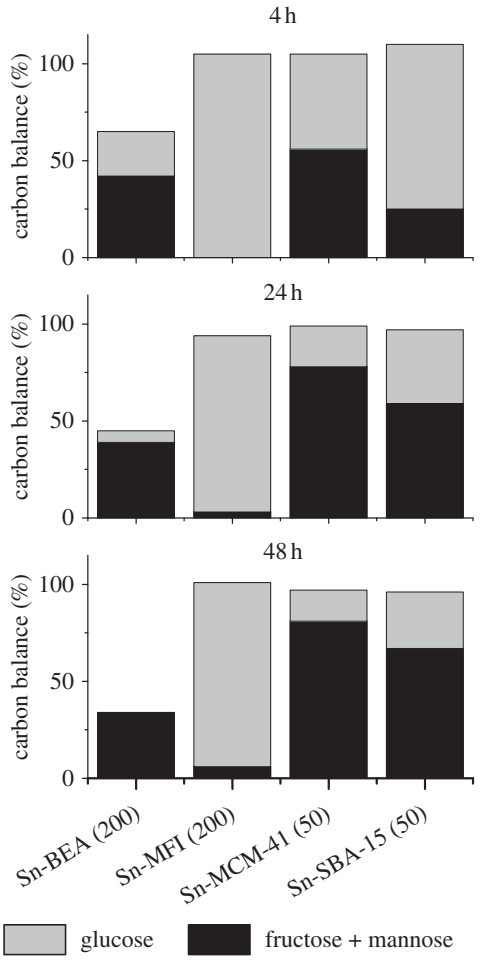

Figure 11. Distribution between hexose sugars after isomerization at 80°C in methanol.

Sn-MFI could be explained by severe diffusion limitations caused by the narrow pore system and the large crystal size. A similar explanation does, however, not hold for the mesoporous stannosilicates, where diffusion should not be a limiting factor. It could instead be caused by deactivation of the active sites by interaction with water. The active sites in the BEA zeolite, and for that matter in the MFI, will be more resistant to deactivation from water owing to the highly hydrophobic nature of the catalyst (Corma *et al.* 2003). Owing to the amorphous nature and large pore system of the mesoporous stannosilicates, a similar effect would not be observed for these.

To examine this further, we attempted to perform the isomerization in methanol (figure 11). Again, Sn-BEA displayed the highest activity, in this case reaching a maximum yield of 42 per cent within 4 h. However, in this case, conversion of hexoses to other compounds was significant, lowering the hexose mass balance to only 65 per cent at this reaction time. At longer reaction times, the mass balance was lowered further, to a point where only fructose and mannose were detected in the reaction mixture. This indicates that ketoses

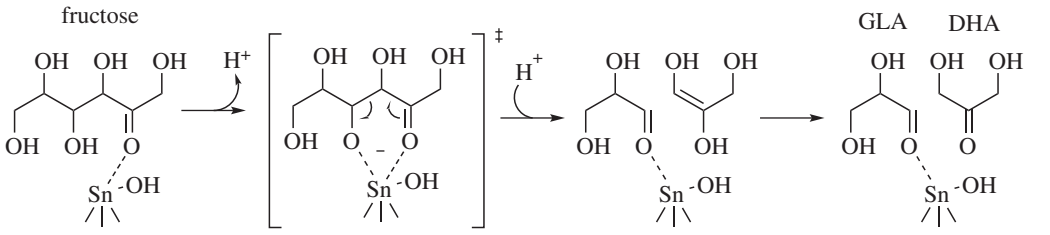

Figure 12. Tentative reaction mechanism for the stannosilicate-catalysed retro aldol condensation of fructose to triose sugars.

are significantly more stable than aldoses under these conditions. The significant decrease in hexose mass balance observed with Sn-BEA was not observed with the mesoporous stannosilicates, thus at longer reaction times higher yields of the isomerization products were obtained; Sn-MCM-41 gave a yield of approximately 75 per cent with no significant loss of hexoses after 17 h, while Sn-SBA-15 appears to approach a similar yield, although at a much slower rate. It thus appears that the deactivation of the active sites observed in water does not occur in methanol. Similarly to the results from the reaction run in water, Sn-MFI gave negligible conversion. Since Sn-MFI was demonstrated to efficiently catalyse the isomerization of trioses, the low conversion with the larger hexose substrate strongly indicates that the reaction is hampered by diffusion limitations.

The use of hexose sugars as the substrate for the production of methyl lactate (reaction scheme given in figures 6 and 12) is significantly more interesting owing to the lower cost of the feedstock compared with triose sugars, although it is also significantly more challenging; a number of alternative reaction pathways are possible, most notably dehydration to furanoic compounds and polymerization reactions leading to insoluble by-products, both of which lower the overall yield of methyl lactate significantly. The catalysts were tested for their activity in the conversion of sucrose to methyl lactate; the yields are given in figure 13. Again, Sn-BEA gives significantly higher yields—more than double the yield of the other catalysts. It is interesting to note the lack of difference between the other catalysts, all of them giving slightly more than 20 per cent yield. This further emphasizes the lack of correlation between the number of tin atoms in the structure and the number of active sites. The yield obtained using Sn-MFI is in fact surprisingly high; the size of the substrate, even after scission of the disaccharide to the constituent hexoses, will impose severe diffusion limitations, compounded by the size of the zeolite crystals. It is possible that the reaction only occurs at active sites located at the surface of the crystals or in the pore mouths.

Characterization of the catalyst used for the conversion of sucrose after regeneration showed no significant change in pore volume of the zeolite catalysts, as shown in table 2; however, the mesoporous stannosilicates lost a significant amount of their pore volume and BET surface area. This could simply be due to the deposition of carbon species in the pore system, which could not be removed by the regeneration procedure employed; however, since this procedure was identical for all catalysts, it seems more likely that the mesoporous structures are less stable at the conditions used for the hexose conversion. The stability of the zeolites and the mesoporous stannosilicates has previously been demonstrated, albeit at lower temperatures, in that the yield obtained with the catalysts did not

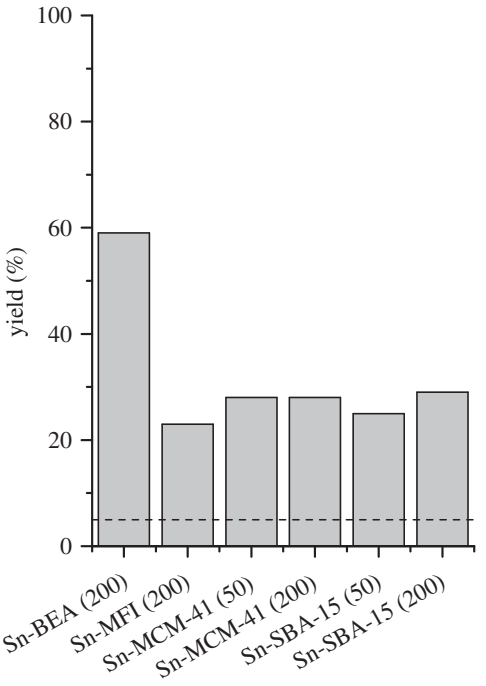

Figure 13. Obtained yield of methyl lactate from the conversion of sucrose at 160°C in methanol. The yield is calculated as the fraction of carbon atoms of the substrate that were incorporated in the product. The dashed line is the yield obtained using Si-BEA.

Table 2. Characterization of used catalyst after regeneration and elemental analysis of reaction liquid.

	pore system retention		
sample	BET area (%)	pore volume (%)	leaching Sn (%)
Sn-BEA (200)	100	100	5.9
Sn-MFI (200)	101	100	3.7
Sn-MCM-41 (50)	84	80	1.5
Sn-MCM-41 (200)	88	88	4.1
Sn-SBA-15 (50)	79	82	3.2
Sn-SBA-15 (200)	95	80	8.4

decrease upon re-use (Holm *et al.* 2010; Li, L. *et al.* 2011). This does not, however, conclusively demonstrate the stability of the active sites, as numerous factors influence the observed yield (Sheldon *et al.* 1998). To investigate the stability, the amount of metal which had leached into the reaction liquid was determined by elemental analysis. Significant amounts of tin species were present in the liquid, irrespective of the structure, and although this could possibly be partly ascribed to catalyst particles small enough not to be retained by the filtration or to the soluble extra-framework tin species, it indicates that the incorporated tin sites are not stable at the employed reaction temperature in liquid media. Previous

studies on similar materials have concluded that the active metal does not leach (Corma & Renz 2004; Li, L. *et al.* 2011); however, these were performed at lower temperatures, which could explain the discrepancy. To test whether leached tin species displayed catalytic activity, an experiment was performed where Sn-BEA was heated to 160°C in methanol for 3 h, and then removed by filtration. The substrate was added to the liquid and the reaction allowed to proceed. The yield obtained was identical to the blank run, thus the leached species are not catalytically active and the catalysis is truly heterogeneous; however, the loss of active sites draws the long-term stability of the catalysts, under these conditions, into question.

4. Conclusion

Stannosilicates have great potential as catalysts for use in a future biomass-based chemical industry, owing to the diverse range of reactions that can be catalysed with high activity and selectivity. Significantly different catalytic properties are, however, observed between structures, which cannot simply be explained by differences in diffusion properties. Thus, the type of structure influences the nature of the active site. This can be directly observed by measuring the change in vibrational frequency of a probe molecule adsorbed onto the active site. Sn-beta possesses an active site with a significantly higher acid strength than the other catalysts investigated; a difference that is probably responsible for the high catalytic activity at low temperature, as observed for the conversion of triose sugars into methyl lactate. In the conversion of hexose substrates, significantly higher yields of methyl lactate were obtained with Sn-beta. Thus, for the production of lactic acid, none of the other catalysts tested can match the activity and selectivity of Sn-beta. The high strength of the active site is, however, not necessarily an advantage, as observed when attempting to isomerize glucose, since alternative reactions begin to dominate at elevated temperatures. This could of course be compensated for by lowering the reaction temperature; however, this may not be desirable as the yield is limited by thermodynamics and a lower temperature would lead to a lower equilibrium yield (Moliner *et al.* 2010). Instead, matching the strength of the active site to favour the desired reaction can be done by choosing a different structure, and the range of structures can be thought of as a toolbox, where the optimal structure differs between applications. Further investigation of the influence of the structure on the active site is necessary, and, in particular, insights into the cause of the difference, on an atomic level, would be of great importance. The perspective of tailoring the active site to the desired application is exciting, and could potentially significantly improve the selectivity of these stannosilicate catalysts.

The Catalysis for Sustainable Energy initiative is funded by the Danish Ministry of Science, Technology and Innovation.

References

Boronat, M., Concepción, P., Corma, A., Renz, M. & Valencia, S. 2005 Determination of the catalytically active oxidation Lewis acid sites in Sn-beta zeolites, and their optimisation by the combination of theoretical and experimental studies. *J. Catal.* **234**, 111–118. (doi:10.1016/j.jcat.2005.05.023)

Boronat, M., Corma, A. & Renz, M. 2006*a* Mechanism of the Meerwein-Ponndorf-Verley-Oppenauer (MPVO) redox equilibrium on Sn and Zr-beta zeolite catalysts. *J. Phys. Chem. B* **110**, 21 168–21 174. (doi:10.1021/jp063249x)

Boronat, M., Corma, A., Renz, M. & Viruela, P. M. 2006*b* Predicting the activity of single isolated Lewis acid sites in solid catalysts. *Chem. Eur. J.* **12**, 7067–7077. (doi:10.1002/chem.200600478)

Boronat, M., Concepción, P., Corma, A. & Renz, M. 2007 Peculiarities of Sn-Beta and potential industrial applications. *Catal. Today* **121**, 39–44. (doi:10.1016/j.cattod.2006.11.010)

Boronat, M., Concepción, P., Corma, A., Navarro, M. T., Renz, M. & Valencia, S. 2009 Reactivity in the confined spaces of zeolites: the interplay between spectroscopy and theory to develop structure-activity relationships for catalysis. *Phys. Chem. Chem. Phys.* **11**, 2876–2884. (doi:10.1039/b821297j)

Christensen, C. H., Rass-Hansen, J., Marsden, C. C., Taarning, E. & Egeblad, K. 2008 The renewable chemicals industry. *ChemSusChem* **1**, 283–289. (doi:10.1002/cssc.200700168)

Corma, A. & Renz, M. 2004 Sn-beta zeolite as diastereoselective water resistant heterogeneous Lewis-acid catalyst for carbon-carbon formation in the intramolecular carbonyl-ene reaction. *Chem. Commun.* **2004**, 550–551. (doi:10.1039/b313738d)

Corma, A., Domine, M. E., Nemeth, L. & Valencia, S. 2002 Al-free Sn- Beta zeolite as a catalyst for the selective reduction of carbonyl compounds (Meerwein-Ponndorf-Verley reduction). *J. Am. Chem. Soc.* **124**, 3194–3195. (doi:10.1021/ja012297m)

Corma, A., Domine, M. E. & Valencia, S. 2003 Water-resistant solid Lewis acid catalysts: Meerwein-Ponndorf-Verley and Oppenauer reactions catalyzed by tin-beta zeolite. *J. Catal.* **215**, 294–304. (doi:10.1016/S0021-9517(03)00014-9)

Corma, A., i Xamena, F. X. L., Prestipino, C., Renz, M. & Valencia, S. 2009 Water resistant catalytically active Nb and Ta isolated Lewis acid sites, homogeneously distributed by direct synthesis in a Beta zeolite. *J. Phys. Chem. C* **113**, 11 306–11 315. (doi:10.1021/jp902375n)

de la Torre, O., Renz, M. & Corma, A. 2010 Biomass to chemicals: rearrangement of β-pinene epoxide into myrtanal with well-defined single-site substituted molecular sieves as reusable solid Lewis-acid catalysts. *Appl. Catal. A* **380**, 165–171. (doi:10.1016/j.apcata.2010.03.056)

Fan, W., Fan, B., Shen, X., Li, J., Wu, P., Kubota, Y. & Tatsumi, T. 2009 Effect of ammonium salts on the synthesis and catalytic properties of TS-1. *Microporous Mesoporous Mater.* **122**, 301–308. (doi:10.1016/j.micromeso.2009.03.018)

Gandini, A. 2008 Polymers from renewable resources: a challenge for the future of macromolecular materials. *Macromolecules* **41**, 9491–9504. (doi:10.1021/ma801735u)

Hayashi, Y. & Sasaki, Y. 2005 Tin-catalyzed conversion of trioses to alkyl lactates in alcohol solution. *Chem. Commun.* **2005**, 2716–2718. (doi:10.1039/b501964h)

Holm, M. S., Saravanamurugan, S. & Taarning, E. 2010 Conversion of sugars to lactic acid derivatives using heterogeneous zeotype catalysts. *Science* **328**, 602–605. (doi:10.1126/science.1183990)

Janssen, K. P. F., Paul, J. S., Sels, B. F. & Jacobs, P. A. 2007 Glyoxylase biomimics: Zeolite catalyzed conversion of trioses. *Stud. Surf. Sci. Catal.* **170**, 1222–1227. (doi:10.1016/S0167-2991(07)80981-5)

Li, L., Stroobants, C., Lin, K., Jacobs, P. A., Sels, B. F. & Pescarmona, P. P. 2011 Selective conversion of trioses to lactates over Lewis acid heterogeneous catalysts. *Green Chem.* **13**, 1175–1181. (doi:10.1039/c0gc00923g)

Li, P., Liu, G., Wu, H., Liu, Y., Gang Jiang, J. & Wu, P. 2011 Postsynthesis and selective oxidation properties of nanosized Sn-beta zeolite. *J. Phys. Chem. C* **115**, 3663–3670. (doi:10.1021/jp1076966)

Mal, N. K., Ramaswamy, V., Rajamohanan, P. R. & Ramaswamy, A. V. 1997 Sn-MFI molecular sieves: synthesis methods, 29Si liquid and solid MAS-NMR, 119Sn static and MAS NMR studies. *Microporous Mater.* **12**, 331–340. (doi:10.1016/S0927-6513(97)00081-3)

Moliner, M., Román-Leshkov, Y. & Davis, M. E. 2010 Tin-containing zeolites are highly active catalysts for the isomerization of glucose in water. *Proc. Natl Acad. Sci. USA* **107**, 6164–6168. (doi:10.1073/pnas.1002358107)

Nikolla, E., Román-Leshkov, Y., Moliner, M. & Davis, M. E. 2011 'One-pot' synthesis of 5-(hydroxymethyl)furfural from carbohydrates using tin-beta zeolite. *ACS Catal.* **1**, 408–410. (doi:10.1021/cs2000544)

Pereira, C. S. M., Silva, V. M. T. M. & Rodrigues, A. E. 2011 Ethyl lactate as a solvent: properties, applications and production processes: a review. *Green Chem.* **13**, 2658–2671. (doi:10.1039/c1gc15523g)

Ragauskas, A. J. *et al.* 2006 The path forward for biofuels and biomaterials. *Science* **311**, 484–489. (doi:10.1126/science.1114736)

Ramaswamy, V., Shah, P., Lazar, K. & Ramaswamy, A. V. 2008 Synthesis, characterization and catalytic activity of Sn-SBA-15 mesoporous molecular sieves. *Catal. Surv. Asia* **12**, 283–309. (doi:10.1007/s10563-008-9060-6)

Román-Leshkov, Y., Moliner, M., Labinger, J. A. & Davis, M. E. 2010 Mechanism of glucose isomerization using a solid Lewis acid catalyst in water. *Angew. Chem. Int. Ed.* **49**, 8954–8957. (doi:10.1002/anie.201004689)

Sasidharan, M., Kiyozumi, Y., Mal, N. K., Paul, M., Rajamohanan, P. R. & Bhaumik, A. 2009 Incorporation of tin in different types of pores in SBA-15: synthesis, characterization and catalytic activity. *Microporous Mesoporous Mater.* **126**, 234–244. (doi:10.1016/j.micromeso.2009.05.038)

Selvaraj, M. & Choe, Y. 2010 Well ordered two-dimensional SnSBA-15 catalysts synthesized with high levels of tetrahedral tin for highly efficient and clean synthesis of nopol. *Appl. Catal. A* **373**, 186–191. (doi:10.1016/j.apcata.2009.11.014)

Serrano-Ruiz, J. C. & Dumesic, J. A. 2009 Catalytic upgrading of lactic acid to fuels and chemicals by dehydration/hydrogenation and C-C coupling reactions. *Green Chem.* **11**, 1101–1104. (doi:10.1039/b906869d)

Sheldon, R. A., Wallau, M., Arends, I. W. C. E. & Schuchardt, U. 1998 Heterogeneous catalysts for liquid-phase oxidations: philosophers' stones or trojan horses. *Acc. Chem. Res.* **31**, 485–493. (doi:10.1021/ar9700163)

Taarning, E., Saravanamurugan, S., Holm, M. S., Xiong, J., West, R. M. & Christensen, C. H. 2009 Zeolite-catalyzed isomerisation of triose sugars. *ChemSusChem* **7**, 625–627. (doi:10.1002/cssc.200900099)

Taramasso, M., Perego, G. & Notari, B. 1983 *Preparation of porous crystalline synthetic material comprised of silicon and titanium oxides.* US Patent no. 4,410,501.

Thomas, J. M., Raja, R. & Lewis, D. W. 2005 Single-site heterogeneous catalysts. *Angew. Chem. Int. Ed.* **44**, 6456–6482. (doi:10.1002/anie.200462473)

Thomas, J. M., Hernandez-Garrido, J. C. & Bell, R. G. 2009 A general strategy for the design of new solid catalysts for environmentally benign conversions. *Top. Catal.* **52**, 1630–1639. (doi:10.1007/s11244-009-9302-5)

Valencia, S. & Corma, A. 2001 *Stannosilicate molecular sieves.* US Patent no. 6,306,364 B1.

Vennestrøm, P. N. R., Osmundsen, C. M., Christensen, C. H. & Taarning, E. 2011 Beyond petrochemicals: the renewables chemicals industry. *Angew. Chem. Int. Ed.* **50**, 10 502–10 509. (doi:10.1002/anie.201102117)

West, R. M., Holm, M. S., Saravanamurugan, S., Xiong, J., Beversdorf, Z., Taarning, E. & Christensen, C. H. 2010 Zeolite H-USY for the production of lactic acid and methyl lactate from C3-sugars. *J. Catal.* **269**, 122–130. (doi:10.1016/j.jcat.2009.10.023)

Zehui, Z. & Zongbao, Z. K. 2011 Hydroxyapatite Lewis acid catalysts for the transformation of trioses in alcohols. *Chin. J. Catal.* **32**, 70–73. (doi:10.1016/S1872-2067(10)60162-3)

Zhu, Y., Chuah, G. & Jaenicke, S. 2004 Chemo- and regioselective Meerwein-Ponndorf-Verley and Oppenauer reactions catalyzed by Al-free Zr-zeolite beta. *J. Catal.* **227**, 1–10. (doi:10.1016/j.jcat.2004.05.037)